

## BEARING CHARACTERISTICS OF CONCRETE IN COMPOSITE STRUCTURE

Md. Khasro Miah\*<sup>1</sup> and A. S. M. Morshed<sup>2</sup>

<sup>1</sup> Professor, Department of Civil Engineering, DUET, Bangladesh, e-mail : [mkhasro@duet.ac.bd](mailto:mkhasro@duet.ac.bd)

<sup>2</sup> Senior Structural Engineer, Bureau Veritas (Bangladesh) Pvt. Ltd., Bangladesh, e-mail : [morshed235@yahoo.com](mailto:morshed235@yahoo.com)

### ABSTRACT

*In the steel-concrete hybrid structural system such as the bridge and building hybrid structures, stud shear connector is one of the key elements, which connects the steel and concrete member as well as transfer the shear force from one member to another member. To provide the constitutive relation of the bearing springs, the bearing characteristics is used, which is investigated under the monotonic and pulsating loads. A series of bearing tests was carried out to observe the bearing characteristics under the monotonic and pulsating loads employing 100mm studs having  $\phi 13\text{mm}$ ,  $\phi 16\text{mm}$  and  $\phi 20\text{mm}$  diameter. Data logger and Visual Log Software were used for recording the experimental responses. Experimental responses obtained from monotonic load are compared with those obtained from pulsating load for the specimens with different sizes of stud. Test results show that specimen under monotonic load undergoes larger displacement than that of the specimen under pulsating load. Specimen with smaller size ( $\phi 13\text{mm}$ ) stud carries less bearing capacity in comparison with specimen with relatively larger size ( $\phi 16\text{mm}$  or  $\phi 20\text{mm}$ ) stud.*

**Keywords:** Composite structure, shear connector, bearing characteristics, monotonic load, pulsating load

### 1. INTRODUCTION

Nowadays, in the developed country the structural system referred to as the steel-concrete hybrid structure (Chinn, 1965; Goble, 1968) is frequently adopted in the construction of buildings and bridges, even in the regions of high seismic risk areas. Steel-concrete hybrid structure has been used since early 1920s. It gained widespread uses in bridges in 1950s and in buildings in 1960s (Ollgaard, Slutter and Fisher, 1971). Steel-concrete hybrid structure is composed of the composite structure and the mixed structure. Hybrid steel and concrete elements can have different forms. Examples include the steel girder with concrete slab, concrete pier with steel girder, steel framing of a building with the concrete floor slabs, the encasement of a steel element with concrete, or the filling of a steel hollow section with concrete.

The hybrid elements can be used to transfer shear force between the two materials to realize the benefits of hybrid action. Benefits can include an increase in strength and stiffness as well as the restraint of buckling instabilities in the steel or confinement of concrete. Hybrid action can be achieved through mechanical connection between the steel and concrete members in composite structure. Due to increasing traffic demand, the number of bridges is increasing rapidly in the developed as well as developing countries all over the world. In this regard, considering the high speed traffic movement and long span bridges, composite bridge structure (Mainstone and Menzies, 1967), is one of the key resources to solve the traffic demand. For the composite bridges, appropriate shear connectors (Hawkins and Mitchell, 1984; Lloyd and Wright, 1990) need to connect the steel and concrete members for allowing the composite action. The headed studs are commonly used as the shear connectors in all type of the steel-concrete composite and mixed structures belong to the hybrid structures. The stud shear connectors are subjected to various types of shear forces, for instances monotonic, pulsating and alternating shear forces depending on the source of excitation viz. traffic movement, earthquake excitation or temperature change.

In the steel concrete composite girder bridges or building structures, the studs are employed to transfer the shear force from concrete slab to steel girder or vice versa. The interface behavior between the stud shear connector and the surrounding concrete, defined here as the bearing characteristics is the key interest of this investigation. To evaluate the stud capacity, strain and displacement behavior along the height of the stud shear connector numerically, bearing springs need to be incorporated for modeling the stud along with the steel girder. To provide the constitutive relation of the bearing springs, the bearing characteristics is used, which is investigated under the monotonic and pulsating loads.

From the literature survey it has been observed that different researchers investigated the static behavior as well as the fatigue behavior of the stud shear connectors with either push-out test or beam test from different perspective. Most of the research works were carried out on stud strength either experimentally or proposed empirical formulae for the pulsating load. The stud strength under monotonic load appears sometimes. The investigation on interface behavior of stud shank and the surrounding concrete is investigated (Miah, Saiki and Nakajima, 2004) only by using  $\phi 13\text{mm}$  stud.

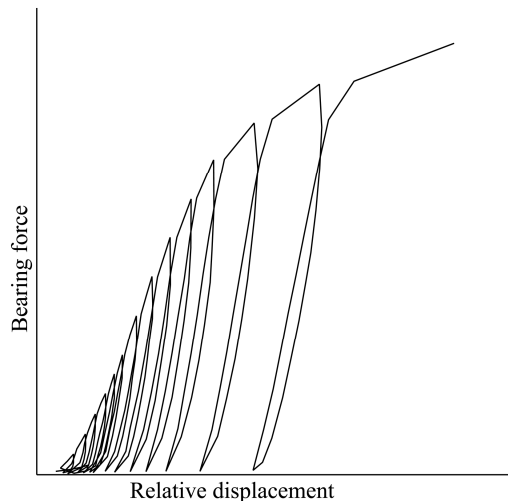


Figure 1: Bearing force-displacement relation

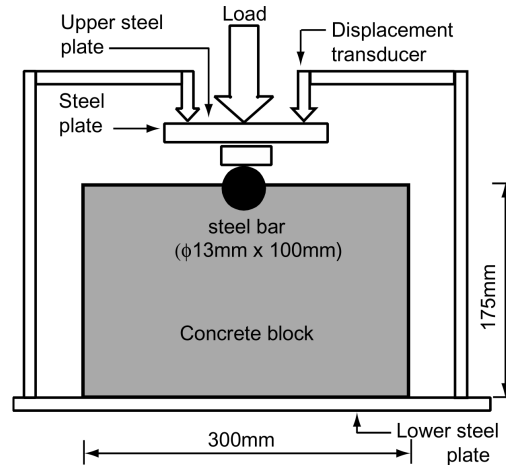


Figure 2: Typical bearing test specimen

To estimate the stud shear capacity at the base, strain behavior along the length of the stud shank numerically, the bearing characteristics is important for modeling the bearing springs. The typical bearing characteristics investigated by Miah, Saiki and Nakajima (2004) with  $\phi 13\text{mm}$  stud only is shown in Figure 1 under pulsating load and the corresponding bearing test specimen is shown in Figure 2. In this study three different size studs viz.  $\phi 13\text{mm}$ ,  $\phi 16\text{mm}$  and  $\phi 20\text{mm}$  (Morshed, 2009) were employed to observe the effect of stud diameter on bearing strength under monotonic and pulsating loads.

## 2. EXPERIMENTAL INVESTIGATION

Experimental investigation was carried out on 22 (twenty two) specimens under monotonic and pulsating loads. Three different size studs viz.  $\phi 13\text{mm}$ ,  $\phi 16\text{mm}$  and  $\phi 20\text{mm}$  were employed. The experimental investigation may be divided into three phases. The first phase consisted of general tests to determine the physical properties of constituent materials like cement, fine aggregate, coarse aggregate, rebar and design of concrete mix to obtain a desired concrete strength. The second phase involved casting of specimens in the laboratory and curing them for 28 days. The third phase comprised of testing specimens to failure to observe the overall behavior under monotonic and pulsating loads. ACI Concrete Mix Design was used to calculate the mix proportion of coarse aggregate, fine aggregate and cement.

20mm down graded crush stone chips was used as coarse aggregate. The unit weight, specific gravity under Saturated Surface Dry (SSD) condition, and absorption capacity of the stone chips were  $1598.30\text{kg/m}^3$  (99.7pcf), 2.62 and 0.43% respectively. The coarse aggregate was properly washed to remove dust and dried up before using in the preparation of concrete.

Coarse sand from Sylhet passing No. 4 sieve was used as the fine aggregate in preparing the concrete mix. The sand was sieved to screen out any unusual particles through sieve No. 4. The sand was washed with water and air dried before use. The unit weight was  $1574.5\text{kg/m}^3$  and specific gravity under SSD condition was 2.62. The fineness modulus of fine aggregate was determined following ASTM C 136-88 (1988) and it was 2.40.

Ordinary Portland cement was used as binding material for the preparation of fresh concrete. Locally produced Holcim (Blue) band cement was used. It was free from lumps, adulteration and /or partial setting. Three cube specimens of 50.8mm size were tested as per ASTM C109-84 (1984) to get compressive strength of cement used in casting of test specimens. The standard sand recommended by ASTM C778-84 (1984) was used for making cement and mortar. The mortar strength at 28 days was  $19.3\text{MPa}$  (2800psi). Unit weight of cement was  $1475\text{kg/m}^3$  (92pcf).

Water used for casting purpose was free from impurities like oil, grease, organic and chemical matters. Water available in the laboratory is of portable quality which is supplied from deep tube well of DUET and is known to have no unusual impurities.  $\phi 13\text{mm}$ ,  $\phi 16\text{mm}$ ,  $\phi 20\text{mm}$  diameter mild steel bars are used as stud in bearing test specimens. Three samples of 16mm, 20mm, and 22mm diameter each were selected for tension test to ascertain the physical properties of steel. The average yield and ultimate strength based on nominal diameter was found to be 385MPa and 542MPa for  $\phi 16\text{mm}$ , 360MPa and 532MPa for  $\phi 20\text{mm}$  and 361MPa and 533MPa for  $\phi 22\text{mm}$  respectively. Deformed mild steel bars of diameter 16mm, 20mm and 22mm respectively were employed to make  $\phi 13\text{mm}$ ,  $\phi 16\text{mm}$  and  $\phi 20\text{mm}$  plane bar after grinding which were used as stud in bearing test specimen.

The mix proportions 1: 2.50: 3.33 by weight and water cement ratio (0.35) were used for the preparation of test specimens and accompanying control cylinders of  $\phi 150\text{mm}$  ( $\phi 6''$ ) were cast to observe the 28 days crushing strength. The slump of the fresh concrete ranged between of 50mm to 54mm for the different days specimen castings. Water cured cylinders were tested after 28 days to observe the strength variations as the test specimen were cured in room temperature. The compressive strength of the accompanying cylinders was recorded by standard cylinder test according to ASTM 39-88 (1988).

The bearing test specimen as shown in Figure 3 was employed to conduct the bearing test for observing the bearing characteristics. The size of the bearing test specimens was 300mm x 175mm x 150mm. The bearing test specimen is extracted from the push-out test specimen (Figure 2) or push and pull-out test specimen as shown in Figure 4. The length of stud was 100mm, half of which was embedded inside the concrete block as shown. Three different diameters viz.  $\phi 13\text{mm}$ ,  $\phi 16\text{mm}$ , and  $\phi 20\text{mm}$  were used to verify the effect of diameters on bearing capacity. The formwork for the test specimens was made of steel plate forming the base and boundaries. The boundary plates and angles were either welded or fastened with nut and bolts to make the desired specimens dimensions.

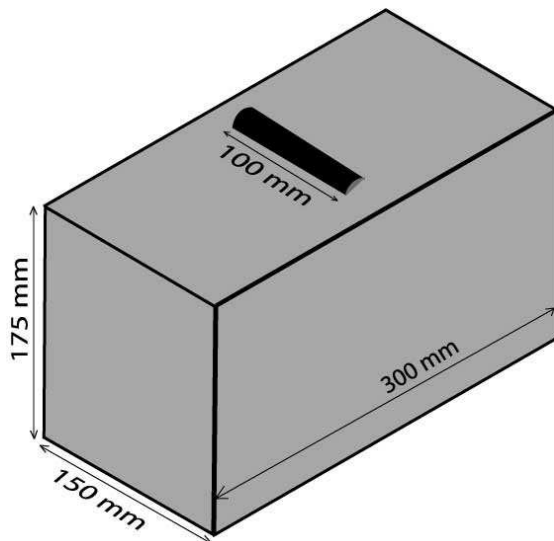


Figure 3: Typical bearing test specimen

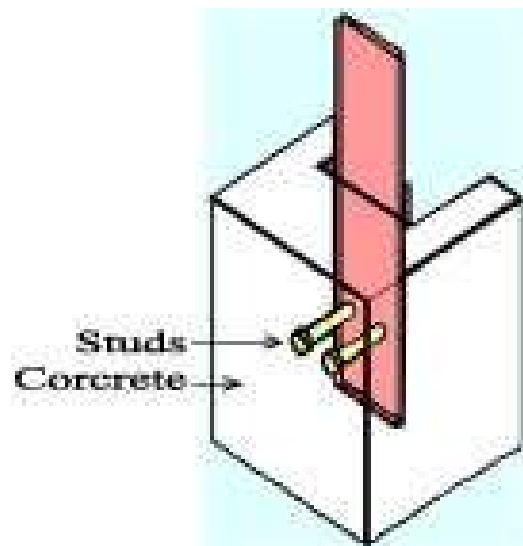


Figure 4: Push and Pull-out test specimen

The test specimen was placed on lower crosshead of the Universal Testing Machine as shown in Figure 5. Two steel plates of size 300mm x 75mm were placed orthogonally to each other on stud, half of which was embedded inside the concrete. A plate of size 150mm x 150mm x 16mm was then placed on the top of 300mm x 75mm plates. A load cell of model no. CLC-NA-1MNA as shown in Figure 5 was followed by another 150mm x 150mm x 16mm plate at its top. Then the upper crosshead was set in contact of the plate at the top of load cell. Finally load was applied from the control panel. Displacements were recorded at some pre-selected points as shown Figure 5 by means of electrical displacement transducers positioned at the top of two steel plates placed as shown, which were placed on the stud of the test specimen. Four displacement transducers were fastened at pre-selected locations in order to make average. The failure pattern of the specimen after experimental investigation is shown in Figure 6.



Figure 5: Loading arrangement (LA)

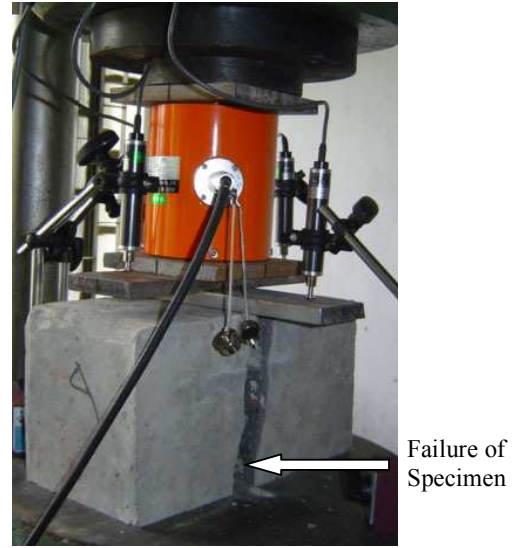


Figure 6: Failure mode of test specimen

Initially a small amount of load was applied to check the effectiveness of the load cell and the contact between the needle of the displacement transducer and plate placed on the stud. The load was then completely removed. After that the initial zero load readings for the load cell, displacement transducers were taken. Two types of loadings viz. monotonic and pulsating loadings were applied on the specimen.

The experiment was carried out on the twenty-two specimens. Ten of those were employed for pulsating loading and the rest twelve specimens were arranged for the monotonic loading. In case of the monotonic load, the test was continued by applying the load at suitable increment of 5kN until failure of the specimen. The readings of the load cell and displacement transducers were automatically saved in the computer at 5kN interval and displayed the load-displacement relations at the pre-selected location graphically. At the same time the data or responses were printed out from Data Logger. The ultimate stage was assumed to have been reached when the displacement transducer readings progressively increased without any significant change in the applied load. On the other hand, in case of the pulsating load, the test was continued by applying unidirectional cyclic loading (compressive) at suitable increment of 5kN with different peak loads. The pulsating compressive loading cycles were repeated with several incremental peak loads up to 300kN. Then the load was increased monotonically up to the failure of the specimen. The same procedure of applying either monotonic or pulsating load was adopted for the specimens having studs diameter of  $\phi 13\text{mm}$ ,  $\phi 16\text{mm}$  and  $\phi 20\text{mm}$ .

### 3. TEST RESULTS AND DISCUSSIONS

A total of twenty two bearing test specimens having dimension of 300mm x 175mm x 150mm were tested, each of which was loaded with either monotonic load or pulsating load. Three types of studs viz.  $\phi 13\text{mm}$ ,  $\phi 16\text{mm}$  and  $\phi 20\text{mm}$  were used in the test scheme. Among the twenty two bearing test specimens, seven specimens were cast with  $\phi 13\text{mm}$  stud, nine specimens were cast with  $\phi 16\text{mm}$  stud and rest ones were cast with  $\phi 20\text{mm}$  stud. The twenty two bearing test specimens may be divided into three major groups depending on stud diameters and each group again subdivided based on loading types like monotonic and pulsating in Table 1. The 28-days average crushing strength of accompanying cylinders and average bearing capacity of each subgroup are also provided in Table 1.

#### 3.1 Bearing Force at the Contact Surface

The load applied on the stud half of which was embedded in concrete block of the bearing test specimen is resisted by concrete bearing force. The bearing force system at the contact surface along with the applied load is shown in Figure 7. The concrete bearing force acts as normal to the embedded surface of the stud shank as shown, the horizontal components of which are minimized because of equal and opposite sign and only the vertical components are exist. Therefore, the bearing capacity of the concrete around the embedded portion of the stud shank is the summation of vertical component only. Since, the dimension (300mm x 175mm x 150mm) of concrete block was same for the all specimen, the effect of concrete block size was not investigated.

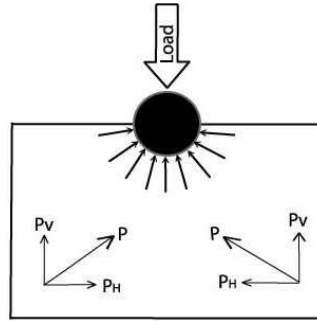


Figure 7: Bearing force system at contact surface

All of the specimens with studs either  $\phi 13\text{mm}$  or  $\phi 16\text{mm}$  or  $\phi 20\text{mm}$  were failed in the fashion of split type like tensile test failure of concrete cylinder along and near center line of the stud as shown in Figure 7. The following data were recorded for each of the test specimen during experiment.

- (i) Displacements at four numbers of locations on the top of stud by applying either monotonic or pulsating load at suitable increment of 5kN.
- (ii) Bearing capacity of concrete at failure under monotonic or pulsating loads

The bearing capacity of concrete is defined as the failure load of the specimen, which one is expressed here as load per unit length. The experimental data were carefully recorded and examined to study the behavior of test specimens. The experimental setup of the bearing test specimen is shown in Figure 7. The experimental responses were used to plot the bearing force versus corresponding displacement curves. The experimental responses are plotted according to the grouping of the test specimens. The behavior and experimental observation of each of the test specimen is discussed here.

### 3.2 Bearing force-displacement relations

The experimental observations related to the bearing force and corresponding displacement of all specimens under monotonic load as well as pulsating load is discussed here. The bearing force-displacement relations under monotonic load along with pulsating load of the specimens with  $\phi 13\text{mm}$  stud are shown in Figure 8. The dashed line indicates the relation under monotonic load and solid line indicates the relation under pulsating load, the ordinate of which indicates the bearing force and abscissa indicates the corresponding displacement. Similarly, the bearing force-displacement relations of all the specimens with  $\phi 16\text{mm}$  and  $\phi 20\text{mm}$  studs under monotonic and pulsating loads are shown in Figure 9 and Figure 10 respectively that the best fit curve of the average values under monotonic load are agree with the outlines of the curve of the relation under pulsating load.

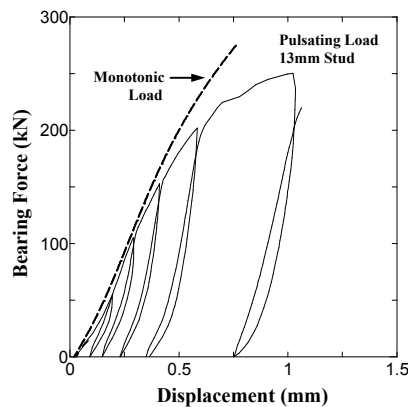


Figure 8: Bearing force-displacement relations ( $\phi 13\text{mm}$  stud)

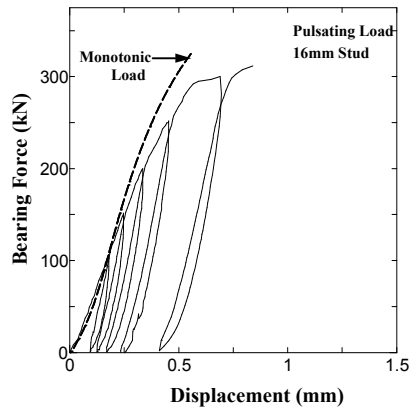


Figure 9: Bearing force-displacement relations ( $\phi 16\text{mm}$  stud)

From the comparison between  $\phi 16\text{mm}$  and  $\phi 20\text{mm}$  studs, the displacement at any particular level of applied load is relatively larger for the specimen with  $\phi 16\text{mm}$  stud because of less contact surface area. Similarly, in

case of  $\phi 13\text{mm}$  and  $\phi 16\text{mm}$  studs, the displacement at any particular level of applied load is relatively larger for the specimen with  $\phi 13\text{mm}$  stud. Therefore, in Figure 8 or Figure 9 or Figure 10, the displacements at any level of applied load in the specimens with  $\phi 20\text{mm}$ ,  $\phi 16\text{mm}$  and  $\phi 13\text{mm}$  studs respectively follow the increasing order as the contact surface area between the stud shank and the surrounding concrete gradually decreasing. The relation under monotonic load resembles and agrees with the outline curve under pulsating load. The displacement at any load level under monotonic load is smaller than the one under pulsating load. This is because of cumulative plastic deformation of the surrounding concrete of stud shank during cyclic loading.

Table 1: Bearing capacity of test specimen (average)

Specimen Size	Group No.	Sub group	Diameter of Studs	Loading Types	28-Days Cylinder Crushing Strength, MPa (psi)	Bearing Capacity, N/mm (lb/inch)
300mm x 175mm x 150mm	#1	1A	$\phi 13\text{mm}$	Monotonic	33.0 (4780)	2620 (14907)
		1B		Pulsating	34.4 (4990)	2270 (12915)
	#2	2B	$\phi 16\text{mm}$	Monotonic	33.0 (4780)	3020 (17182)
		2A		Pulsating	28.6 (4150)	2690 (15305)
	#3	3A	$\phi 20\text{mm}$	Monotonic	36.3 (5265)	3570 (20311)
		3B		Pulsating	33.0 (4780)	3130 (17808)

In the case of pulsating load, the test was continued by applying unidirectional cyclic loading (compressive) at suitable increment of 5kN with different peak loads. The pulsating compressive loading cycles were repeated with several incremental peak loads up to 300kN. In Figure 8, it is observed that the stiffness of the loading and unloading path is about 950kN/mm on average, while it is clear about 500kN/mm initially because of plastic deformation. The plastic deformation of the surrounding concrete of stud shank is making progress due to increasing the peak values of cyclic loading. In Figure 9 specimen with  $\phi 16\text{mm}$  stud, the stiffness of the loading and unloading path is about 1500kN/mm approximately, whereas initially is about 600kN/mm. Similarly, the stiffness of the loading and unloading path is about 750kN/mm on average, whereas initially is about 250kN/mm of the specimen having  $\phi 20\text{mm}$  stud in Figure 10. The initial and average stiffness of the bearing force-displacement relation in Figure 10 is smaller than the one as shown in Figure 9. This is the reason why the displacement of relation indicated by dotted line in Figure 11 at any level of applied load smaller than the one indicated by dashed line or solid line. The three bearing force-displacement relations of the specimens with  $\phi 13\text{mm}$ ,  $\phi 16\text{mm}$  and  $\phi 20\text{mm}$  studs under pulsating load are compared in Figure 11.

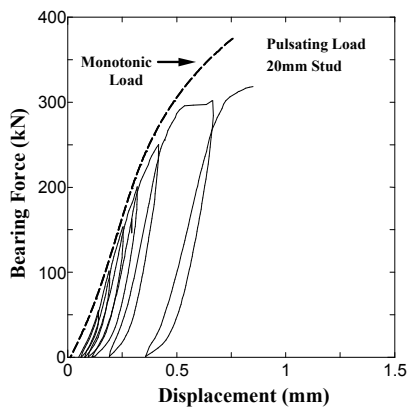


Figure 10: Bearing force-displacement relations ( $\phi 20\text{mm}$  Stud)

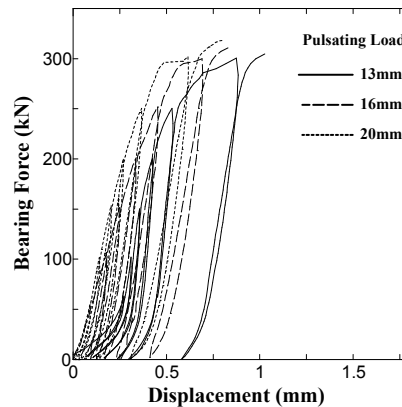


Figure 11: Bearing force-displacement relations (All)

### 3.3 Bearing Capacity under Monotonic and Pulsating Loads

The bearing capacity of concrete is defined the maximum load at which the failure of the specimen occurred. The average bearing capacity of concrete according to grouping of the test specimens is shown in Table 1. The

bearing capacity of concrete depends upon the surface area of the stud embedded in concrete block. In this regard, specimen with smaller diameter stud will carry smaller bearing capacity, which one agrees according to Table 4.1. The average bearing capacity of concrete of test specimen with  $\phi 13\text{mm}$ ,  $\phi 16\text{mm}$  and  $\phi 20\text{mm}$  studs are found 2620 N/mm (14907 lb/inch), 3020 N/mm (17182 lb/inch) and 3570 N/mm (20311 lb/inch) respectively under monotonic loading. For pulsating loading, the average bearing capacity of concrete of test specimen with  $\phi 13\text{mm}$ ,  $\phi 16\text{mm}$  and  $\phi 20\text{mm}$  studs are found 2270 N/mm (12915 lb/inch), 2690N/mm (15305 lb/inch) and 3130 N/mm (17808 lb/inch) respectively. The bearing capacity of the concrete depends on the contact surface area between the stud shank and the surrounding concrete. The contact surface area with  $\phi 13\text{mm}$  stud is less in comparison with  $\phi 16\text{mm}$  or  $\phi 20\text{mm}$  stud exhibit less bearing capacity of concrete. Considering specimens with  $\phi 13\text{mm}$  stud, the bearing capacity under monotonic load is greater than the one under pulsating load. During cyclic loading, the capacity of the specimen obviously reduced because of energy dissipation, which was not present in uni-directional monotonic loading. This behavior agrees with the specimens having three types ( $\phi 13\text{mm}$ ,  $\phi 16\text{mm}$  and  $\phi 20\text{mm}$ ) of studs in Table 1.

#### 4. CONCLUSIONS

The following conclusions may be drawn based on the observation of the experimental study carried out in this research program.

- (i) Specimen with smaller size stud ( $\phi 13\text{mm}$ ) undergoes larger displacement than the specimen with larger size stud ( $\phi 16\text{mm}$  or  $\phi 20\text{mm}$ ) for the same applied load.
- (ii) Specimen with same size stud shows smaller displacement under monotonic load than the one under pulsating load.
- (iii) The outline of the bearing force-displacement relation under pulsating load agrees with the bearing force-displacement relation under monotonic load.
- (iv) The bearing capacity of concrete increases with increase in the contact surface area of stud in concrete block.
- (v) The bearing capacity of concrete under monotonic load is higher than that under pulsating load.

#### ACKNOWLEDGEMENTS

The authors wish to thank the department of Civil Engineering, Dhaka University of Engineering & Technology (DUET) for providing all sorts of cooperations in laboratories to complete the research work in due time. This work was financially supported by the department of Civil Engineering of DUET.

#### REFERENCES

- Chinn, J. (1965), "Push out tests on lightweight composite slabs", Engineering Journal, AISC, Vol.2 (4), pp. 129-134.
- Goble, C. (1968), "Shear strength of thin flange composite specimen", Engineering Journal, AISC, Vol. 5(2), pp. 62-65.
- Hawkins, N.M. and Mitchell D. (1984), "Seismic response of composite shear connections", Journal of Structural Engineering, ASCE, Vol. 110, No.9, pp. 2120-2136.
- Lloyd, R. M. and Wright, H. D. (1990), "Shear connection between composite slabs and steel beams", Journal of Construction Steel Research, Vol. 15(2), pp. 255-285.
- Mainstone, R. J. and Menzies, J. B. (1967), "Shear connectors in steel-concrete composite beams for bridges", part-1: Static and Fatigue Tests on Push out Specimens, Concrete, London, England Vol. 1, No. 9, pp. 291-302.
- Miah, M. K., Saiki, I. and Nakajima, A. (2004), "Numerical evaluation of static behavior of stud shear connectors", JSCE Journal of Applied Mechanics, Vol. 7, pp. 571-578.
- Ollgaard, J. G., Slutter, R. G., and Fisher, J. W. (1971), "Shear strength of stud connectors in lightweight and normal-weight concrete", Engineering Journal, AISC, 8(2), pp. 55-64.
- Morshed, A. S. M. (2009), "Investigation of the Bearing Characteristics of concrete in Composite Structure", Master of Engineering Thesis, Department of Civil Engineering, Dhaka University of Engineering and Technology, Gazipur.